Super hydrophobic SAM modified electrodes for enhanced current limiting properties in intrinsic conducting polymer surge protection devices

Noor H Jabarullah,[1,4] Emanuele Verrelli,[1] Clayton Mauldin,[2] Luis A Navarro,[2] Josh H Golden,[2] Leonidas M Madianos[3] and Neil T Kemp[1,*]

1. Department of Physics and Mathematics, University of Hull, Hull, United Kingdom, HU6 7RX
2. TE Connectivity, Menlo Park, California, 94025 USA
3. Department of Physics, National Technical University of Athens, 15780 Zografou, Greece
4. Electrical Engineering, International College of Engineering, University Kuala Lumpur, British Malaysian Institute

Email: n.kemp@hull.ac.uk

Abstract. Surface interface engineering using super hydrophobic gold electrodes made with 1-dodecanethiol self-assembled monolayer (SAM) have been used to enhance the current limiting properties of novel surge protection devices based on the intrinsic conducting polymer, polyaniline doped with methane sulfonic acid. The resulting devices show significantly enhanced current limiting characteristics, including current saturation, fold-back and negative differential effects. We show how SAM modification changes the morphology of the polymer film directly adjacent to the electrodes leading to the formation of an interfacial compact thin film that lowers the contact resistance at the Au-polymer interface. We attribute the enhanced current limiting properties of the devices to a combination of lower contact resistance and increased joule heating within this interface region which during a current surge produces a

current blocking resistive barrier due to a thermally induced de-doping effect caused by the rapid diffusion of moisture away from this region. The effect is exacerbated at higher applied voltages as the higher temperature leads to stronger depletion of charge carriers in this region resulting in a negative differential resistance effect.

1. Introduction

Recently we reported a new type of low-cost two terminal resistive current limiting device for use in low and medium power surge protection.[1] The device, which is based upon a single material consisting of a thin-film of an intrinsic conducting polymer, is distinctly different from conventional surge protection devices, which are instead based upon a composite matrix material of semiconductor (carbon, borides, silicides) or metallic particles embedded within an insulating polymer of high thermal expansion coefficient (polyethylene, epoxy).[2,3] These polymeric positive temperature coefficient (PPTC) devices operate by having many conduction pathways[4,5] that break during a current surge due to joule heating and subsequent thermal expansion of the insulating polymer.[6,7] The resulting high resistance state reduces the current to safe levels, providing protection for components in the circuit and other attached electrical equipment. In contrast, our intrinsic conducting polymer devices operate via a mechanism of partial de-doping of the polymer films caused by the diffusion of water out of the polymer film due to a joule heating process. The single component system has the advantages of low cost starting materials and inexpensive method of fabrication.

Whilst our previously reported devices showed current saturation behaviour at higher voltages the devices did not show current foldback behaviour, which occurs when the current reaches a maximum value and then decreases with increasing applied voltages (see Figure 1, curve B). Current foldback has the advantage that the current is not only limited but is as well reduced, thereby minimizing potential damage to the device and any external circuits for which the device serves to protect. In this paper we demonstrate that surface interface engineering using superhydrophobic self-assembled monolayers (SAM) leads to current foldback and negative differential resistance effects in our surge protection devices. In some cases almost complete suppression of the current is observed.

Interface engineering of organic semiconductor – metal interfaces is of high current interest as it is provides an important tool for modifying charge transport characteristics in devices. In particular controlling the contact resistance is important for modifying charge injection/extraction in organic LEDS, photovoltaics and thin-film transistors.[8] Ohmic contacts can be achieved when the highest occupied molecular orbital (HOMO) or lowest unoccupied molecular orbital (LUMO) level of the bulk organic material are closely aligned with the Fermi energy of the metal, thereby allowing injection or extraction of charge with a small or negligible energy barrier. In this respect the use of a thin, highly ordered two-dimensional layer of polar molecules that self-assemble on a metal electrode to form a dipole in the desired direction can improve the alignment of the energy levels as it shifts the work function of the metal.[9] SAMs of straight chain hydrocarbons and SAMs with different functional groups have been used to modify the work function of various metals e.g. Au,[10] Cu,[11] and metal oxides e.g. ITO[12, 13] and it has been shown that fine-tuning of the work function can be achieved through the use of the SAMs with differing dipoles, e.g. hexadecanethiol and perfluorinated alkanethiols, which having opposite dipoles, can respectively decrease and increase[14] the work function of Ag (Φ_{Ag} ~ 4.4eV) to 3.8 and 5.5 eV.

The use of SAMs for surface engineering is proving to be an important technique for modifying charge injection/extraction in conjugated polymer based devices. Phosphonic acid based SAMS have yielded particularly promising results, improving charge injection and electroluminescence in polymer LEDs,[15] whilst in polymer diodes[16] they have been used to tailor the performance of devices through modification of the internal electric field and built-in potential (V_{BI}). Fluorinated phosphonic acid SAMs of 1H,1H,2H,2H-Perfluorooctanephosphonic acid (FOPA) have also been used to increase the work function of ITO from 4.8 eV to 5.3 eV, giving decreased contact resistance, greater hole injection, enhanced incident-photon-to-current conversion efficiency (IPCE), higher on/off ratio and wider detector dynamic range in organic photodetectors based on fluorine-type conjugated polymers.[17] Other types of SAMS have also been investigated. A novel series of silane-tethered bis(fluoroaryl) amine SAMs, having the advantages of high resistance to chemical and thermal degradation, have been used

to improve charge extraction in organic photovoltaics devices.[18] Newly synthesized ionic SAMs, consisting of an anchoring group, a linker group, and an ionic functional group have been used on source/drain electrodes in polymeric semiconductor thin film transistors.[19] The devices showed 50% lower contact resistance, resulting in more efficient hole injection into the active channel. In a new development[20] the use of heterogeneous SAMs, consisting of a mixture of both small and long chain-length alkyls, have shown significant improvement in charge selectivity and collection in organic photovoltaics due to the increased headgroup density, which causes additional band bending and favourable alteration of the Schottky barrier height.

In this work we have used SAM modified electrodes to alter the contact resistance at Au – conducting polymer polyaniline interfaces so as to improve the current limiting properties of surge protection devices. SAM modification of the interface between metal and doped intrinsically conducting polymers have been much less studied, although several studies have used SAMs as charge blocking layers to facilitate patterning at the micron[21, 22, 23] and nano[24, 25, 26] length scales during electrochemical deposition of the polymer. To the best of our knowledge we have found only one study in the literature that has investigated SAM modified electrodes to change the contact resistance between metal electrodes and electrochemically deposited conducting polymers. This work, using a different SAM, 4-aminothiophenol, showed that SAMs can be used to considerably reduce the contact resistance between the metal electrode and electrochemically deposited polyaniline ($HClO_4$ doped) due to improved binding of the polymer to electrode.[27] This was attributed to better adhesion (covalent bond) of the SAM to the Au electrode due to the high affinity of thiols to gold. Modification of the contact resistance by non-SAM techniques has also been investigated. Techniques include direct doping of the polymer layer,[28] surface doping via the incorporation of an dopant molecule on the metal electrodes prior to deposition of the polymer by spin-coating,[29] graft polymerization[30] and incorporation of buffer layers[31] (e.g. poly(ethylenedioxythiophene) / poly(styrene sulfonic acid) [PEDOT : PSS] or LiF) between the metal and polymer material so as to add a step between the Fermi level of the metal and HOMO level of the polymer.

2. Materials and Device Preparation

The conducting polymer current limiter device used in this study is similar to that previously reported.[1] The devices consists of a thermally insulating ceramic substrate with two top-deposited gold electrodes (4-6 μm thick) that are separated by a 55 μm gap containing the conducting polymer. The conducting polymer, polyaniline doped with methane sulfonic acid, is electrochemically deposited onto the gold electrodes using a bath consisting of 0.5 M polyaniline (Aldrich, 99.5%) and 2.0 M methane sulfonic acid (MSA) (Aldrich, 99.5%) in de-ionized water. The polymer has a nanofibre spaghetti-like morphology with a high surface area to volume ratio. More details of the device fabrication and deposition process as well as the methods used for electrical testing of the devices can be found in our earlier publication.[1]

SAM modification of the gold electrodes was performed prior to deposition of the polymer. The procedure involved leaving the devices for up to 72 hrs in an ethanol solution with 0.01 M of 1-dodecanethiol (DDT) $C_{12}H_{26}S$ (Aldrich, >98%). The SAM's were characterised using drop shape analysis using a Kruss DSA10 equipped with a CCD camera. The advancing and receding angle technique demonstrated a contact angle of 152°, Figure 2 (inset), indicating the formation of a superhydrophobic surface. Figure 2 shows the polymerisation current during the electrochemical deposition of polyaniline for the non-SAM and SAM modified electrode devices. In contrast to the 55 s deposition time of non-SAM devices, SAM devices needed longer deposition times of 110 s due to the current blocking behaviour of the self-assembled monolayer.[32] This observed strong current blocking effect along with the results from the drop shape analysis, indicating the formation of a superhydrophobic surface, as well as electrical studies on devices with different DDT concentrations and exposure times (see Figure 6) indicate high quality formation of the SAM on the gold electrodes.

3. Results

Fast I-V sweeps (10 V/s) were used to simulate the conditions of a current surge. Multiple sweeps were performed from zero and ranging up to a maximum voltage of 5 - 10 V. Between each sweep the device

was allowed to recover for 1 minute to allow the device to reset back to its original starting resistance. Figure 3a) shows the typical I-V characteristics for a single non modified device in ambient air (approx. 70% relative humidity) with sweeps to increasingly higher maximum voltages. Each sweep shows non-linear current limiting behaviour at high voltages leading to increased device resistance. A measure of the current limiting behaviour of the device can be made by comparing the current at 10 V with the ohmic response current on the graph (straight line). At 10 V the current has been reduced by 40%.

In contrast the I-V characteristics for a self-assembled modified (SAM) device are shown in Figure 3b). In this case the I-V curves show much greater current limiting behaviour. This is particular evident at voltages above 5 V where negative differential resistance and current fold back properties are observed, characteristics which have not been previously observed with previous device. A comparison of the current at 10 V to the ohmic response (straight line) indicates a much larger reduction in the current, 85%, more than double of that observed for the non-SAM devices.

Previously we have shown that moisture plays a critical role in the current limiting properties of the devices thus studies were also carried out in a controlled environment with different relative humidity. Figure 4a) and 4b) show a comparison between non-SAM and SAM devices with relative humidity ranging from 10% to 90%. The graph indicates that the current limiting behaviour of the device is dependent upon the relative humidity. For the highest levels of relative humidity, 80% and 90%, the I-V curves clearly show very good current limiting properties with behaviour similar to that of the current saturation in curve B of Figure 1.

Figure 5a) and 5b) show a comparison of the current-voltage properties of a SAM modified device at different humidity levels of 60% and 90% respectively. The current-voltage curves of the sample in the lower humidity environment, Fig. 5a), show reduced current at higher applied voltages. The 7-10 V sweeps all have the same trend whilst the first sweep to 6 V is quite different in that current saturation occurs at a much lower voltage. This has also been seen with other devices of the same type, but not in all cases. As this is only ever seen to occur with the first sweep in the series it is likely to be associated

with the previous history of the device and the initial water content in the film. Fig. 5b) shows the current-voltage properties of a device in a much higher humidity environment (90%). In contrast the device shows much stronger current limiting properties as shown by the current saturation and negative differential resistance at higher applied voltages. This can be attributed to the increased water content in the polymer film because of the more humid environment. The graph also shows that the resistance of the device, taken as the inverse gradient close to the origin, becomes higher as the experiment has progressed from the first sweep at 5 V to the last sweep at 10 V. This is likely due to the polymer needing longer times between sweeps to achieve the same water content prior to the beginning of the experiment, although we note some polymer aging effects have been observed at high applied voltages/currents (see supplementary information S1). The main result from Fig. 5a) and 5b) is that larger current limiting properties are observed in higher humidity environments, as was similarly observed in our previous work[1] on non-SAM modified devices, with the effect being more intense in SAM devices.

Studies were also carried out to investigate the effect of the SAM on the current limiting properties of the devices and to determine the optimum conditions for deposition of the SAM. Figure 6a) shows a plot of the normalized I-V characteristics for a SAM device in ambient air (approx. 70% relative humidity) prepared using a10 mM DDT/ethanol solution and different immersion times of 24, 48 and 72 hrs. The transition from current reduction to current saturation and current foldback (slight) in the I-V characteristics clearly shows that the current limiting properties of devices is enhanced for devices with longer immersion times. Figure 6b) shows the I-V properties of devices prepared instead with different DDT/ethanol concentrations of 1, 5 and 10 mM. These results shows show that enhanced current limiting properties can be achieved with the use of higher DDT concentrations.

To investigate whether polymer morphology was affected because of current blocking properties of the SAM modified gold electrodes, SEM images were taken of the conducting polymer at different times during growth of the polymer. Figure 7a) shows the morphology of the polymer on the SAM modified gold electrode at 25 s and shows how the SAM greatly affects the polymer morphology in the vicinity

of the electrode, producing a compact layer of polymer growth instead of the spaghetti-like growth observed for a non-SAM device. Figure 7b) show that at 55 s the polymer morphology undergoes a transition and the polymer instead deposits with a spaghetti-like morphology. From the SEM images we estimate the compact layer on the SAM device is 1 μm thick. In contrast, devices without a SAM do not have this compact layer. To determine whether this compact layer extends into the channel region along the surface of the Al_2O_3 substrate, thereby possibly influencing current transport between the source and drain electrodes, the cross sectional area of the polymer within the channel region was examined by SEM. Figure 7c) shows a cross-sectional SEM image of the channel region of a fully grown device (110 s). The cross-section interface was prepared by freeze fracturing the device at liquid nitrogen temperature (Note: Au electrodes are to the left and right and the Al_2O_3 substrate is at the bottom). The cross section image shows highly porous spaghetti like growth throughout the channel region with no evidence of the compact layer extending across the surface of the Al_2O_3 substrate. From this we conclude that compact polyaniline thin-film only occurs at the surface of the gold electrode.

The effect of the SAM on the electrical properties of the Au – polymer interface was investigated by measuring the contact resistance of SAM and non-SAM device. To determine the contact resistance a series of devices were made with different gap separations ranging from 10 μm to 100 μm. Figure 8 shows a plot of device resistance (with equivalent film thickness) vs. electrode spacing for SAM and non-SAM devices with differently spaced electrodes. Extrapolation to zero distance electrode separation allows determination of the contact resistance of the devices. The plot indicates that non-SAM devices have a total contact resistance (including both electrodes) of 9.69 Ω whilst SAM devices are significantly lower with 2.55 Ω.

Figure 9 show the results of finite element modelling of joule heating in a) non-SAM and b) SAM devices. The description of the modelling and parameters used are detailed in the section below. The main results from the joule heating modelling show that for devices subject to applied voltages of 2.5 V the SAM devices show much higher temperatures at the polymer – gold interface than for non-SAM devices. Furthermore, because the total current in SAM devices is higher than non-SAM devices (total

resistance of SAM devices R_{SAM} = 4.35 Ω is lower than that of $R_{non\text{-}SAM}$ = 11.3 Ω) the power dissipated in SAM devices is much higher than in non-SAM devices, for the same voltage bias, resulting in higher overall temperatures throughout the device. An estimate of the average power dissipated at 2.5 V from Fig.3 shows that the power dissipated in a SAM device is almost double of that in a non-SAM device i.e. $P_{SAM} = I^2R = 0.425^2 \times 4.35 = 0.79$ W and $P_{non\text{-}SAM} = I^2R = 0.2^2 \times 11.3 = 0.452$ W.

4. Modelling

In this section we describe the modelling method for the joule heating thermal plots shown in Figure 9. For both non-SAM and SAM devices we have used the Comsol® multiphysics software with the joule heating and heat transfer modules to investigate heating in the devices as a function of applied voltage and time. The device geometry used in the modelling was the same as the actual devices and the materials parameters were based on either measured values from our own experimental investigations or accepted literature values.

The model for the non-SAM device consists of the conducting polymer channel positioned between the two gold source/drain electrodes. The contact resistance between both gold electrodes and the conducting polymer (9.69 Ω), from Fig.8, is incorporated into the model as a contact resistivity. In contrast for the SAM device, we have attributed the contact resistance (2.55 Ω), from Fig.8 to include both the metal work function shift (see discussion) and the polyaniline compact thin film (thickness 1 μm) that occurs at the surface of the gold electrodes. This has been done for two main reasons. Firstly, the individual contributions of both effects cannot be distinguished from the contact resistance measured in Fig. 8 since the smallest separation between the electrodes used was 10 μm. To distinguish these contribution, separations much lower than 1 μm would be needed and this is beyond the limits of the method used for the device fabrication in this work. Secondly, we believe that the lower contact resistance is most likely due to the presence of the compact thin film rather than the SAM as this is much thicker (~1 μm) than the SAM (1.8 nm) and represents a larger resistive load. Furthermore, since high applied voltages are used typically incurred during a current surge (we have used 5 – 10 V) the

energy barrier due to the misalignment between the E_F of the metal and the HOMO/LUMO levels would only have a small effect.

The parameters used in the joule heating model include a combination of measured values from our own experimental investigations and common literature values. For a non-SAM device the contact resistance of 9.69 Ω, obtained from Fig.8, was converted to a surface resistivity $\rho_S = R_{C1}A = 19.4\times10^{-8}$ Ω m^2 and used directly in the Joule heating model, where $R_{C1} = y_0/2$ with y_0 being the y-intercept in Fig.8 and $A=6.67\times10^{-3} \times 6 \times 10^{-6}$ m^2 is the surface area of the device electrode. For a SAM device the contact resistance of 2.55 Ω, obtained from Fig.8, was converted to a conductivity $\sigma_C = L / R_{C2}A = 0.20$ S/cm to represent the compact thin-film (of thickness L= 1 μm) that is present at the polymer-SAM-Au interface at each Au electrode. In this case $R_{C2} = y_0/2$ is the contact resistance for *one electrode* with y_0 being the y-intercept in Fig.8. In each case, σ_B = 736 S/m, was used for the electrical conductivity of the polyaniline material in the bulk of the device. This was also calculated from Fig.8 and found to be similar for SAM and non-SAM devices. For the thermal conductivity and heat capacity (constant pressure) of the polyaniline nanofibres we have used literature values[33] of k = 0.55 W/mK and Cp = 1.075 J/gK at 300 K to represent the spaghetti-like polyaniline in the bulk of the device and literature values of k = 0.1 W/mK and Cp = 1.1 J/gK for the compact polyaniline thin-film at the electrode interface. The latter being averaged literature values obtained for 20 μm thick[34] films (k = 0.0795 W/mK), 40 μm thick[35] films (k = 0.14 W/mK) and 110 nm thick[36] films (k = 0.144 W/mK). Values for the density of polyaniline[37] ρ=1.33g/cm^3 and surface emissivity[38] εs = 0.725 were also sourced from the literature. The Al_20_3 substrate material was also included in the model as this importantly acts as large heat sink for dissipation of thermal energy from the channel region. The parameters used for Al_20_3 were k = 27 W/mK, Cp = 0.90 J/gK, ρ = 3.90g/cm^3, ε_r = 9.1 and εs = 0.8. The standard material properties of gold for the metal electrodes were also used. The model developed for both device types incorporated joule heating, heat conduction, radiative effects and convection.

5. Discussion

Previously we reported devices with good current limiting behaviour that exhibited current saturation effects at higher applied voltages. However, these devices did not show current foldback and negative differential resistance effects. We discuss here our new results with SAM modified electrodes and show how engineering of the Au-polymer interface can be used to improve current rectification in devices.

The organosulfur compound 1-dodecanethiol $C_{12}H_{26}S$ was chosen because it's known that simple straight chain alkanethiols with chain length of more than 10 carbon atoms form good ordered self-assembled monolayers on Au[39] and that SAMs can be used to modify the charge injection properties at the organic semiconductor/metal interface, effectively increasing or decreasing the contact resistance at the interface. Drop shape analysis of water on the 1-dodecanethiol self-assembled monolayer modified gold electrode (Fig. 2) shows that we were able to achieve a superhydrophobic surface with an immersion time of 48 hrs in a 10 mM DDT concentration. Although it is known that immersion times of only a few seconds to minutes can achieve dense monolayer coverages the monolayers are not necessarily well-ordered and can contain many gauche defects.[40] The reorganization dynamics to produce good pin-hole free single monolayer coverage is a much slower process and much longer periods of immersion are required. For our gold surfaces we found that the best hydrophobic films were produced with immersion times greater than 24 hrs and that longer immersion times of 72 hrs produced the device with the best current limiting properties (Fig. 6a). This was similarly found in the case of higher DDT concentrations where 15 mM produced the best current limiting properties (Fig. 6b) Interestingly, although the stronger concentrations and longer immersion times produced the best current limiting properties this was not reflected in the contact angle measurements which did not show improvement above 24 hrs immersion times or above 5 mM concentrations. This indicates that higher concentrations and longer immersion times do not increase the hydrophobicity of the surface once it has reached a maximum value but are necessary for fixing minor defects in the SAM, such as pinholes, which are more likely to affect the electronic properties of the device to a greater extent since even

small pinholes would permit a significant amount of current to bypass the interface region when the polyaniline material is present.

The presence of the SAM on the electrode surface at first inhibited the polymerization and deposition of polyaniline on the gold electrodes as shown by the 20-30s induction time in the polymerization current (Fig. 2). However, after this initial current blockage, polymerization proceeded and increased rapidly as the total electroactive area of the electrode is increased with the deposition of the polymer. During the initial blocking stage it is expected that there is first diffusion of oxidized monomers to the vicinity of the electrodes followed by the formation of a dense region of oligomers at the electrode / solution interface. With increased density, supersaturation takes place and polymerisation is expected to occur at isolated pinholes in the SAM, followed by spreading out across the SAM surface, as has been seen for polypyrrole deposited onto hexadecanethiol SAM modified Au.[41] Our growth study work shows that the polymer morphology initially formed on the SAM as a dense compact thin-film (Fig. 7a), which is similar to that found with the electrochemical deposition of poly-3-methylthiophene[42] and poly-3-octylthiophene[43] thin-films on dodecanethiol Au modified electrodes as well as polyaniline on p-aminothiophenol modified Au electrodes.[44] In this case however with increased deposition time there is a transition from 2-D lateral growth to 3-D growth as the morphology changes from being compact to highly porous, consisting of polymer nanofibres with a spaghetti-like appearance and with high conductivity. A similar 2-D to 3-D transition has previously been reported by us for polyaniline on gold electrodes and in this work we showed how once this type of growth is established, polymerisation proceeds very rapidly.[45] From the SEM images (Fig. 7) a general picture emerges for the deposition and morphology of polyaniline on DDT SAM modified electrodes, depicted schematically in Figure 10, consisting of first the deposition of polyaniline within defects in the SAM, followed by the formation of compact thin film (ctf) on top of the SAM (~ 1μm thick) and lastly, a transition to a spaghetti-like morphology of polymer nanofibres.

The current-voltage investigations clearly show that SAM modified devices have greater current limiting properties than un-modified devices. This can be seen in the comparison between an

unmodified and SAM modified device under normal ambient conditions (Fig. 3), as well as for a device in different humidity environments (Fig. 4). In general the current limiting properties of SAM modified devices is greater in higher relative humidity environments and with higher applied voltages (Fig. 5), as was similarly observed for un-modified devices in our previous study.[1] These results agree well with the general mechanism proposed previously for the current switching phenomenon, being due to a partial de-doping/re-doping process caused by the rapid diffusion of moisture out of or into the polymer film during joule heating/cooling.

However, unlike our previous work, the I-V characteristics show distinct foldback behaviour and negative differential resistance effects. To understand this in greater detail we first determined the contact resistance of devices with and without the SAM layer (Fig. 8) and used finite element modelling to investigate the temperature distribution in the device during a current surge (Fig.9). The SAM devices were found to have significantly lower contact resistance, 2.55 Ω, in comparison to unmodified devices, 9.69 Ω. For alkanethiol modified electrodes the finding of lower contact resistance in our devices is in fact opposite to that expected from both theory and previous experimental studies. Previous studies have shown that SAM modification of metal surfaces by alkanethiols shifts the work function of the metal to significantly lower values. For example both dodecanethiol[46] and hexadecanethiol[14] modified electrodes decreased the effective work function of Au respectively from 4.75 eV to 4.29 eV ($\Delta\Phi$ = 0.46 eV) and from 4.9 eV to 4.1 eV ($\Delta\Phi$=0.8eV). The reason being that linear alkanethiols, having a dipole moment that points away from the Au electrode, decreases the vacuum level outside the electrode implying a lower effective work function for the SAM modified Au electrode. This is expected to increase the hole injection barrier, Φ_h, whilst decreasing the electron injection barrier, Φ_e. As was observed in the above two cases this led to an increased contact resistance between the metal and *p*-type organic semiconductor materials due to the increase in barrier height for hole injection. Thus the finding of lower contact resistance in our case means that an additional effect is occurring at the interface.

In the following we examine charge injection into polyaniline in more detail. The conducting emeraldine salt form of polyaniline is obtained by oxidative doping of the leucoemeraldine base (fully reduced form) or by protonation of the emeraldine base (half oxidized form) by doping with protonic acids (H^+A^-). In acid doped polyaniline the majority carriers are holes and as they have a considerably higher mobility than electrons in the material they dominate the conduction properties. Hole transport is expected to take place via a half-filled polaron band,[47] calculated theoretically to be of width 1.1 eV and lying 1.8 eV above the highest fully occupied band and 4.1 eV below the conduction band. This is in general agreement with experimentally determined values[47, 48] of ~1.5 eV for the polaron band and 4.3-4.9 eV for the work function, depending on the dopant type and polymerization conditions.[49] Thus although polyaniline has a large energy difference of 5.9 eV between the conduction band and the highest fully occupied band, conduction can occur in the material via low lying half-filled polaronic states. Using these values we can consider the situation in which the work function of the Au electrode is modified by the SAM. In case of an un-modified Au electrode we can assume the E_F of the Au electrode, having a work function ~4.8 eV, is approximately at the level of the broad polaron band in the polymer since the measured work function of polyaniline is 4.3-4.9 eV and the polaron band is rather broad ~1.1 eV. This is consistent with the current-voltage measurement on our devices as well measurement by others on Au – polyaniline junctions,[50] which typically show ohmic behaviour with no evidence of the formation of a Schottky barrier with rectification. In the case of alkanethiol modified Au electrodes, previous studies have shown the work function shifts to lower energy[46,14] by as much $\Delta\Phi$ = 0.8 eV. This shift increases the barrier height for hole injection into the polymer thus increasing the contact resistance of the interface. However, the broadness of the polaron level may mean this effect is only minor in the case of a SAM modified surface. Much stronger effects have been observed however when the metal is changed and in these cases high work function metals give metal-Pani interfaces that are ohmic, whereas low work function metals form Schottky barriers, as confirmed by experiments on metal-Pani junctions[50] and metal-Pani field effect transistors.[51]

From the above picture it is expected that our dodecanethiol modified devices should have increased the contact resistance with respect to that measured for the unmodified devices. However, the opposite was observed, 2.55 Ω, for the SAM devices in comparison to the unmodified devices being 9.69 Ω. Our studies show that to explain this behaviour changes in the polymer morphology in the vicinity of the electrode must also be taken into consideration. This can explain both the decrease in the contact resistance and the changes in the current limiting properties of the devices. Our SEM results (Fig. 7) show the polymer morphology at the surface of the electrodes is very different from that present in the bulk. The latter having a highly porous spaghetti-like morphology whereas the former being a compact and dense thin-film. The higher polymer density will act to lower the contact resistance since this increases the cross-sectional area, which allows more current to flow. The degree of crystallinity and doping level may also be significantly different in this region, which will additionally contribute to changes in the overall contact resistance of the interface region. Our measurements on the contact resistance cannot separate the individual contributions to the contact resistance from changes in the work function of the metal and polymer morphology at the interface since it is difficult to fabricate devices with spacing between the gold electrodes less than 1um.

Only a few reports exist in the literature for polyaniline doped with MSA with which we can make a comparison with for the electrical conductivity of the polyaniline material in the bulk and compact thin film. Both reports have used chemical methods for polymerization which tend to have different morphologies and lower conductivity.[52] In these reports the room temperature conductivity of Pani-MSA thin-films was measured[53] to be 0.1 S/cm and Pani-MSA with a granular morphology[54] was found to be 0.26 S/m. In contrast the conductivity for our films were σ_C = 0.20 S/cm for the compact thin-film and σ_B = 7.36 S/cm for the bulk material. The conductivity of the compact thin film is similar to literature values for MSA doped polyaniline thin-films whilst our value for the bulk nanofibre material is substantially higher. We note that polyaniline nanofibres prepared by chemical routes and differing dopants typically have conductivities[55, 56] ranging from 0.1 to 33 S/cm, with the highest being polyaniline doped with both potassium biiodate and sodium hypochlorite oxidant with conductivities[57] as high as 112 S/cm. In contrast, the highest conductivity “metallic” polyaniline[58] thin-films have

conductivities as high as 1100 S/cm. Thus we can assume our Pani-MSA nanofibre material has a higher conductivity than the compact thin polymer film at the gold electrodes but is still well on the insulating side of the metal insulator transition.

To consider the effect of the formation of the interfacial compact polyaniline thin film on joule heating in devices Finite Element Modelling using COMSOL® was employed. We examined internal heating in the devices at a time of 0.25s, which is approximately the time at which the device response changes from being linear to non-ohmic as can be seen in Fig's 3a and 3b. Our modelling investigations showed that the change in the contact resistance due to a lowering of the effective work function of the metal electrode alone cannot account for the changes in the current limiting behaviour of the non-SAM and SAM devices. However, by incorporating a compact thin film into the joule heating model for the SAM modified devices significant changes in the distribution of joule heating were observed that can account for the current limiting behaviour. The results in Figure 9 show that for a non-SAM device the temperature in the bulk of the device is significantly higher than at the Au-polymer interface. This is because the Au electrodes and Al_2O_3 substrate act as large thermal sinks, cooling the polymer at the extremities of the film. Although temperatures in the bulk (72 - 82°C) are high enough for polymer de-doping via loss of moisture a significant channel region close to the Al_2O_3 substrates exists at a much cooler temperature (61-62°C) which can act as a conduit through which a large amount of conduction can take place. In contrast for the SAM modified devices a large amount of heat is generated within a 1μm thick region adjacent to the electrode. This region, having much higher temperatures (~165°C) would undergo a significant de-doping effect via loss of moisture since Pani-MSA has typically lost most of its moisture by this temperature (see TGA results[1] for Pani-MSA). Since this region is uniformly positioned around the vicinity of the gold electrodes it acts a large resistive barrier that limits conduction in the device. Thus the heating causes a type of pinch-off effect which leads to a negative differential resistance effect, which is identifiable at high applied voltages where the heating effect is exacerbated. Figure 9 also shows that higher overall temperatures occur in SAM devices. This is because the total resistance of SAM devices (R_{SAM} = 4.35 Ω) is lower than non-SAM device ($R_{non\text{-}SAM}$ = 11.3 Ω) at the same applied voltage i.e. 2.5 V, leading to greater power dissipation in the SAM devices.

The results from our thermal modelling can as well provide some insight into the differences observed between SAM devices in low and high relative humidity environment. Figure 5a and 5b show the current-voltage properties of a SAM modified devices at 60% and 90% relative humidity. Much stronger current limiting properties, including negative differential resistance effects, are observed for the device in the higher humidity environment. Since our thermal modelling data indicates the interface region between the metal and polymer layer plays a dominant role in the charge transport and heating in the device it indicates that increased levels of adsorbed water might be preferentially affecting charge transport in the interface region more than in the bulk polymer material. Since the pinch-off effect is exacerbated when the resistance of the interface region is smaller (SAM devices) it would suggest the enhanced current limiting properties observed at higher humidity levels (Figure 5b) is due to a lower resistance in the interface region. This lower resistance could be from the higher adsorbed water content lowering the effective barrier height for charge injection at the interface, an effect utilized in metal/polymer Schottky diode chemical sensors,[59, 60] or could be due to increased conductivity in the compact thin film polymer layer at the metal interface.

In summary the modelling results indicate that SAM modified devices show a negative differential resistance effect because of increased heating at the polymer - gold interface which leads to strong de-doping in the vicinity of the electrodes and a pinch-off effect in the current across the device. Although higher temperatures typically increases the conductivity of conducting polymers because of the thermally activated hopping mechanism, the special role of water as a partial dopant in polyaniline means that moisture loss has instead a dominant effect.

Stability and endurance of the SAM modified devices was also examined (see supporting information, Fig.S1) as well as their response to high speed, high voltage pulses (see supporting information, Fig.S2). For the endurance testing a series of I-V sweeps over a 24 hour period with fast I-V sweeps (10 V/s) was used to simulate the conditions of a current surge. The delay between current surges was 10 min. The devices showed good stability over the 24 hour period with a slight reduction in the conductivity during the first 10 hours. The response speed of the SAM devices was examined by exposing the devices

to high speed, high voltages pulses using a series of high voltage square wave pulses (2 - 100 V) whilst monitoring the current. The data was used to plot a graph of the normalized resistance vs. time, as shown in Figure S2. The graph shows the response of the devices increases rapidly for pulses of higher voltage i.e. 75 and 100 V whereas in the case of low voltage pulses (2 V), the resistance of the device does not significantly change, indicating the passive nature of the devices under normal operating conditions. In comparison to results on non-SAM devices (previously published) the SAM devices showed a twofold increase in the current limiting resistance and faster response times at 100 V.

5. Conclusions

We have shown that surface interface engineering using super hydrophobic gold electrodes made with 1-dodecanethiol self-assembled monolayer (SAM) can be used to enhance the current limiting properties of novel conducting polymer surge protection devices. The current blocking effect of the SAM during the electrochemical deposition process leads to the formation of a compact thin film at the interface of the gold electrodes which modifies the electrical properties of the devices, resulting in significantly enhanced current limiting properties, including current saturation, fold-back and negative differential effects. We attribute this to a combination of the SAM and the formation of an interfacial compact thin polymer film which acts to lower the device contact resistance by a factor of 4 as well as shifts internal heating in the devices during a current surge towards the devices electrode. The resulting higher temperatures in the compact thin film forms a current blocking resistive barrier due to a thermally induced de-doping effect caused by the rapid diffusion of moisture away from this region. The effect is exacerbated at higher applied voltages as the higher temperature leads to stronger depletion of charge carriers in this region resulting in a negative differential resistance effect.

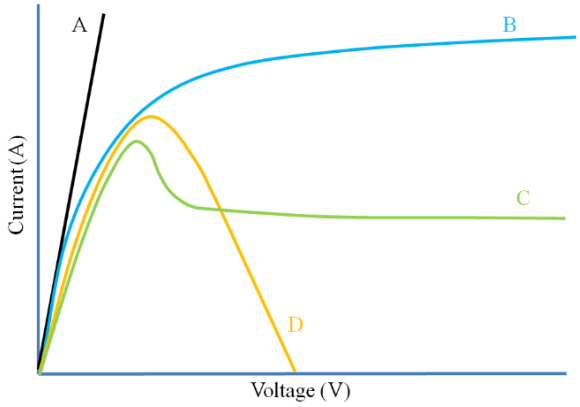

Figure 1. I-V curves showing ohmic behaviour (A), saturation (B), slight foldback (C) and full foldback (D). The idealized I-V properties for circuit and device protection are represented by curves similar to D, however even devices exhibiting the properties of B can be useful for handling high power dissipation. (Reprinted with permission from[1]. Copyright 2014, AIP Publishing LLC.)

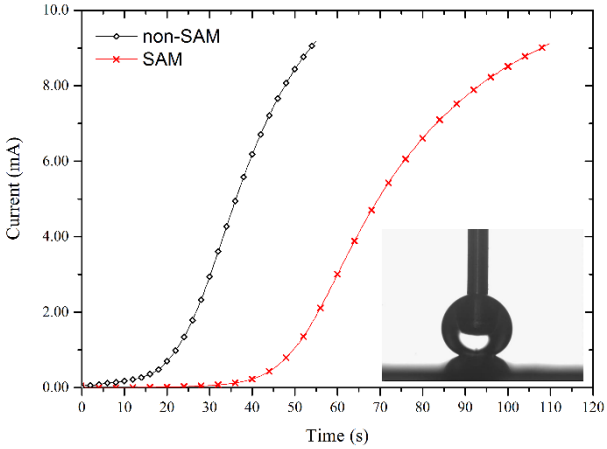

Figure 2: Plot of the deposition current during Pani-MSA electrochemical polymerisation and showing current blocking during the first 30 seconds of the polymerisation on the SAM modified gold electrodes in contrast to gold electrodes with no SAM. Inset shows an image from the drop shape analysis of water on a 1-Dodecanethiol self-assembled monolayer modified gold electrode immersed in a 10 mM concentration of DDT for 48 hrs. Advancing and receding angle technique demonstrated a contact angle of 152°, indicating the formation of a superhydrophobic surface.

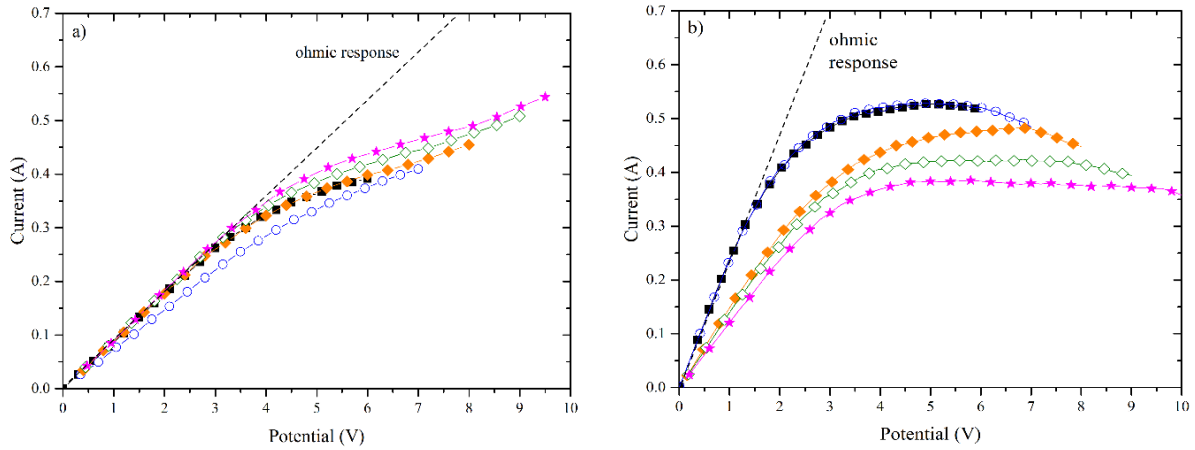

Figure 3. Current-voltage characteristics up to applied voltage of 10 V for a conducting polymer current limiter device in ambient air (approx. 70% relative humidity) with a) with normal gold electrodes (Reprinted with permission from[1]. Copyright 2014, AIP Publishing LLC.) and b) with self-assembled monolayer modified electrodes. For the SAM device the current limiting is greatly enhanced with evidence of both saturation and foldback. The symbols refer to sweeps to 6 V (■), 7 V (blue circle), 8 V (orange rhombus), 9 V (green open rhombus), 10V (pink star). Dashed lines act as guides to the eye for an ohmic response.

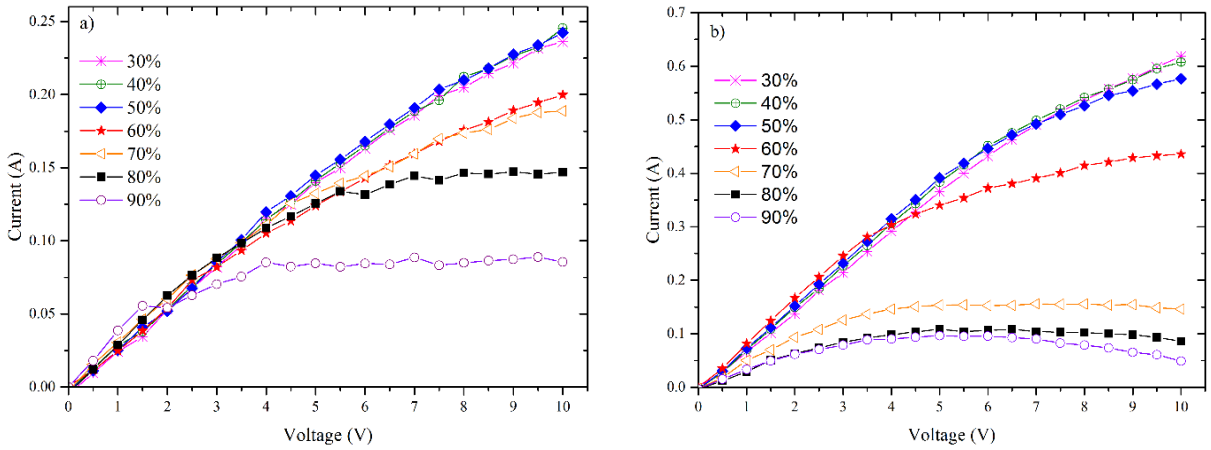

Figure 4. Typical current-voltage characteristics of devices in different humidity environments for a) non-SAM device (Reprinted with permission from[1]. Copyright 2014, AIP Publishing LLC.) and b) a SAM modified device. The SAM modified device shows significantly larger current reduction and negative differential resistance (foldback) above 60% relative humidity.

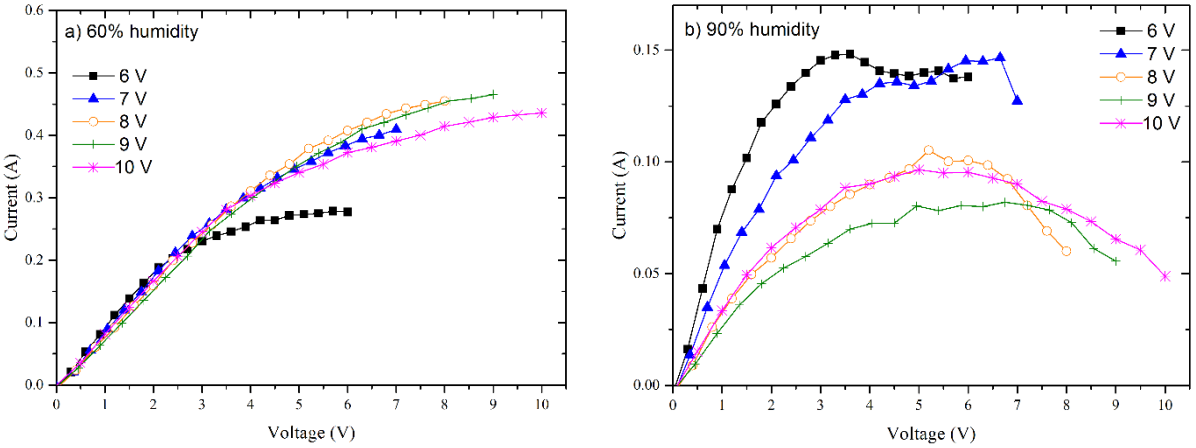

Figure 5. Current-voltage characteristics of a SAM modified device in a) 60% and b) 90% relative humidity environments and showing clear saturation and negative differential resistance current limiting behaviours.

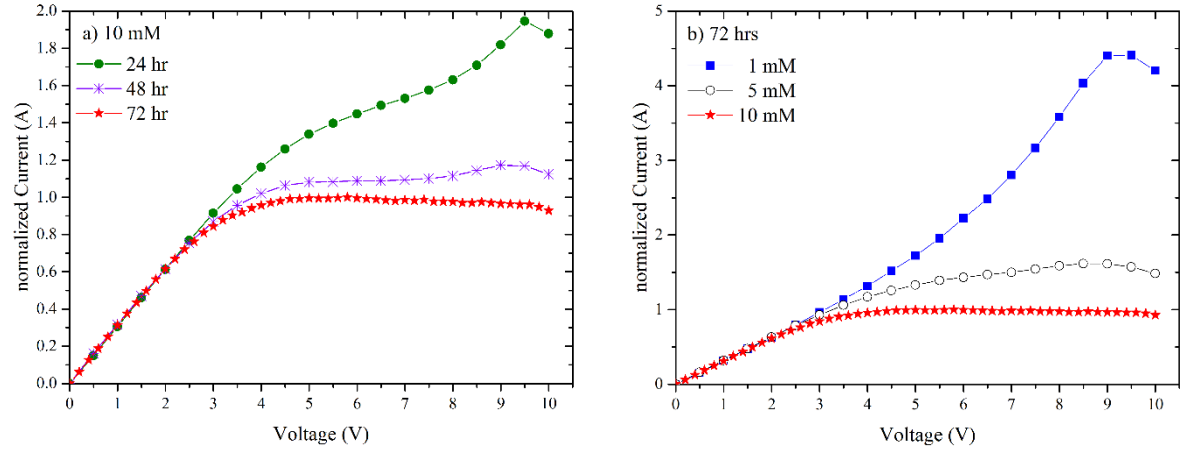

Figure 6. Plot of the normalized Current-Voltage characteristics up to 10 V for a conducting polymer current limiter device in ambient air (approx.. 70% relative humidity) with self-assembled monolayer modified electrodes prepared with a) 10mM concentrated solutions and immersion times of 24 hrs (green circles), 48 hrs (violet cross), 72 hrs (red star) and b) an immersion time of 72hrs with concentrated solutions of 1mM (blue square), 5 mM (black circle) and 10 mM (red star). The graphs show that devices prepared with SAMs having longer immersion times and more concentrated solutions leads to devices with increased current limitation as well as faster response times. (Note: The current values are normalized to have the same starting resistance to allow for different resistances of the devices)

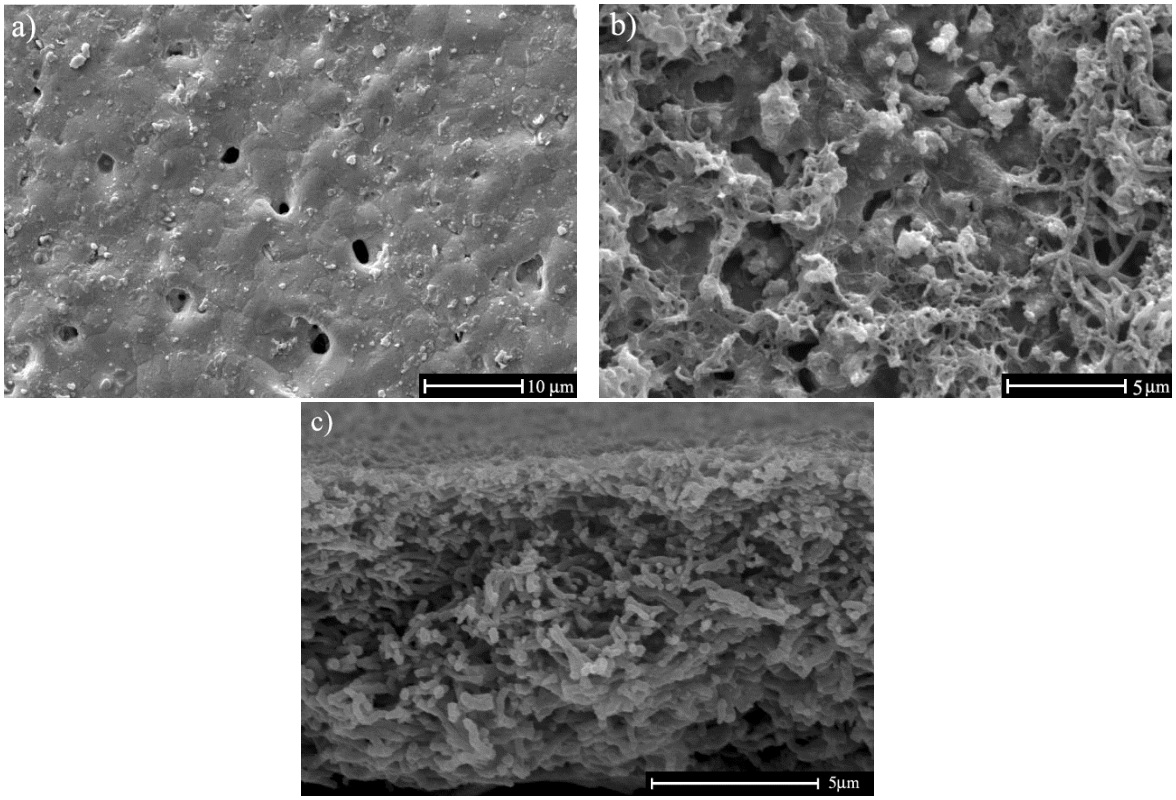

Figure 7. SEM images of polyaniline deposited on SAM modified gold electrode after a) 25s and b) 50s and c) 110s polymerisation time. The images shows that polyaniline initially deposits on the SAM modified electrode as a thin compact layer but as time proceeds changes to a spaghetti-like morphology of polymer nanofibres. In c) the image is taken of a cross section of the channel region between the two gold electrodes for a fully grown film and shows uniform spaghetti-like polyaniline growth throughout the entire film (top to bottom) with no significant change in the polymer morphology close to the Al_2O_3 substrate (bottom). This indicates that the compact polyaniline morphology only occurs at the surfaces of the gold electrode and not in the channel region.

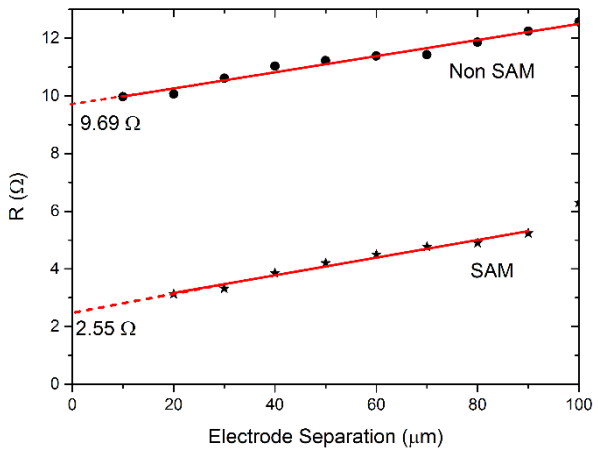

Figure 8. Plot of SAM and Non SAM device resistance vs. electrode spacing for devices with differently spaced electrodes and showing determination of the contact resistance by extrapolating to zero electrode separation. The contact resistance of the SAM device is almost a factor of 4 lower than that of the Non SAM device.

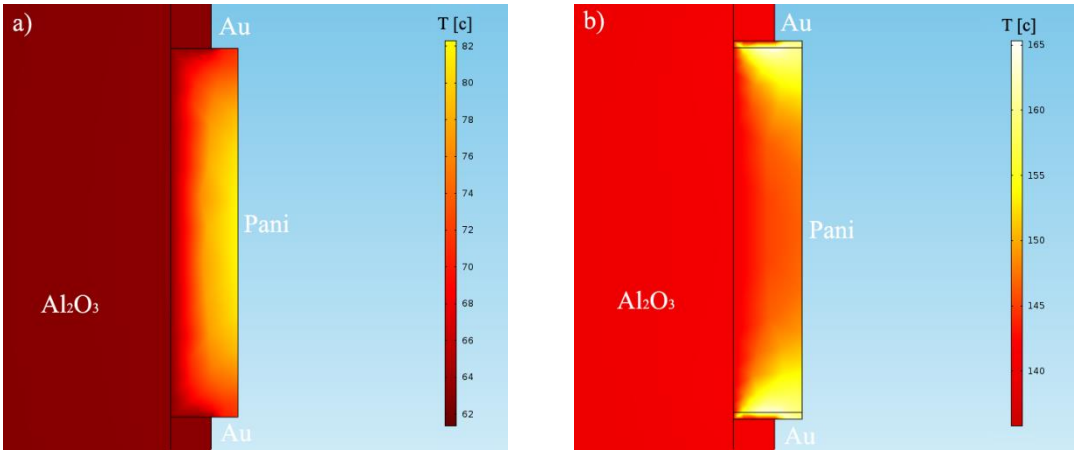

Figure 9. Joule heating model for devices at 2.5 V for a) non-SAM and b) SAM devices and showing higher temperatures at the polymer – gold interface for SAM devices. The overall temperature of the SAM device in the bulk is also much higher due to the lower total device resistance.

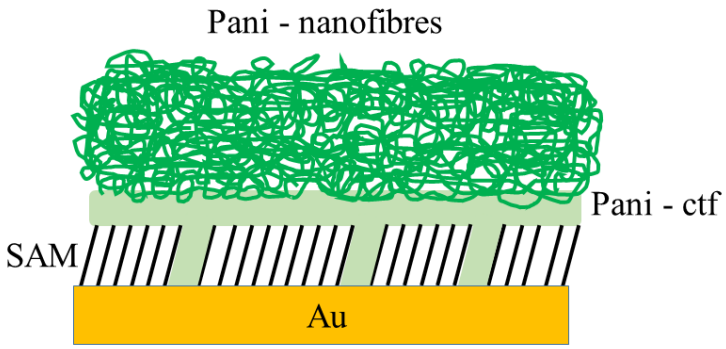

Figure 10. Schematic of the deposition of polyaniline on dodecanethiol SAM modified gold electrodes and showing the initial deposition of the polymer within defects in the SAM, followed by the formation of a compact thin compact thin film (ctf) of thickness 1μm and lastly, the transition to a spaghetti-like morphology of polymer nanofibres.

Acknowledgements We sincerely thank Prof. Dimitris Tsoukalas (Dept. of Physics, National Technical University, Athens), Dr. L. Chen and the Leeds EPSRC Nanoscience and Nanotechnology Research Equipment Facility (LENNF) for technical support and advice on this project as well as Garry Robinson (Dept. of Engineering) and Dr Robert Farley (Dept. of Physics and Maths) at the University of Hull for help with SEM imaging and electronics development.

Supporting Information Available

Stability and endurance of the SAM modified current limiting polymer devices was also examined (Fig.S1) as well as their response to high speed, high voltage pulses (Fig.S2). Please see the supporting information for details on these studies. This information is available free of charge via the Internet at http://pubs.acs.org/.

References

[1] Jabarullah, N. H.; Verrelli, E.; Mauldin, C.; Navarro, L. A.; Golden, J.; Madianos, L.; Tsoukalas, D; Kemp, N. T. Novel Conducting Polymer Current Limiting Devices for Low Cost Surge Protection Applications. *J. Appl. Physics* **2014**, 116, 164501

[2] Pearson, G. Conductive Device. *US Patent No*. 2,258,958 (issued 14 October 1941); *UK Patent Specification* No. 541,222 (issued 18 November 1941)

[3] Frydman, E. Improvements in or relating to resistance elements having positive temperature/resistance characteristics. *UK Patent Specification No.* 604,695 (issued 8 July 1948)

[4] Vernet, S.; Asakawa, G. Regulator Device for Electric Current. *US Patent No*. 2,978,665 (issued 4 April 1961)

[5] Kohler, F. Resistance Element. *US Patent No*. 3,243,753 (issued 29 March 1966)

[6] Ohe, K.; Naito, Y. New Resistor having an Anomalously Large Positive Temperature Coefficient. Jpn. J. Appl. Phys. **1971**, 10, 99

[7] Heaney, M. B. Resistance-expansion-temperature behavior of a disordered conductor-insulator composite. Appl. Phys. Lett. **1996**, 69(17), 2602-2604

[8] Rhee, S. -W.; Yun, D. -J. Metal-semiconductor contact in organic thin film transistors. J. Mater. Chem., **2008**, 18, 5437–5444

[9] Campbell, I. H.; Rubin, S.; Zawodzinski, T. A.; Kress, J. D.; Martin, R. L.; Smith, D. L.; Barashkov, N. N. ; Ferraris, J. P. Controlling Schottky energy barriers in organic electronic devices using self-assembled monolayers. Phys Rev. B, **1996**, 54, 1432-14324

[10] Zehner, R. W; Parsons B. F.; Hsung, R.P.; Sita, L.R. Tuning the work function of gold with self-assembled monolayers derived from X-[C6H4-C C-](n)C6H4-SH (n = 0, 1, 2; X = H, F, CH3, CF3, and OCH3). Langmuir **1999**, 15 (4), 1121−1127

[11] Campbell, I. H.; Kress, J. D.; Martin, R. L.; Smith, D. L. Controlling charge injection in organic electronic devices using self-assembled monolayers. Appl. Phys. Lett. **1997**, 71 (24), 3528-3530

[12] Khodabakhsh, S.; Sanderson, B. M; Nelson, J.; Jones, T. S. Using self-assembling dipole molecules to improve charge collection in molecular solar cells. Adv. Funct. Mater. **2006**, 16(1), 95–100

[13] Khodabakhsh, S.; Poplavskyy, D.; Heutz, S. ; Nelson, J.; Bradley, D. D. D.; Murata H.; Jones, T. S. Using self-assembling dipole molecules to improve hole injection in conjugated polymers. Adv. Funct. Mater., **2004**, 14(12), 1205-120

[14] de Boer, B.; Hadipour, A.; Mandoc, M. M.; van Woudenbergh, T.; Blom, P. W. M. Tuning of metal work functions with self-assembled monolayers. Adv. Mater., **2005**, 17 (15), 621–625

[15] Knesting, K. M.; Hotchkiss, P. J.; MacLeod, B. A.; Marder, S. R.; Ginger, D. S. Spatially Modulating Interfacial Properties of Transparent Conductive Oxides: Patterning Work Function with Phosphonic Acid Self-Assembled Monolayers. Adv. Mater. **2012**, 24, 642−646

[16] MacLeod, B.A.; Horwitz, N.E.; Ratcliff, E.L.; Jenkins, J.L.; Armstrong, N.R.; Giordano, A.J.; Hotchkiss, P.J.; Marder, S.R.; Campbell, C.T.; Ginger, D.S. Built-In Potential in Conjugated Polymer Diodes with Changing Anode Work Function: Interfacial States and Deviation from the Schottky-Mott Limit. J. Phys. Chem. Letts. **2012**, 3(9), 1202-1207

[17] Sato, Y.; Kajii, H.; Ohmori, Y. Improved performance of polymer photodetectors using indium–tin-oxide modified by phosphonic acid-based self-assembled monolayer treatment. Org. Elec. **2014**, 15(8), 1753-1758

[18] Song, C.K.; White, A.C.; Zeng, L.; Leever, B.J. ; Clark, M.D.; Emery, J.D.; Lou, S.J.; Timalsina, A.; Chen, L.X.; Bedzyk, M.J.; Marks, T.J. Systematic Investigation of Organic Photovoltaic Cell Charge Injection/Performance Modulation by Dipolar Organosilane Interfacial Layers. ACS Appl. Mater. Interfaces. **2013**, 5(18), 9224-9230

[19] Lee J.; Park J.S.; Lee, B.-L.; Park J.-i.; Chung, J.W.; Lee. S. Ionic self-assembled monolayer for low contact resistance in inkjet-printed coplanar structure organic thin-film transistors. Org. Elec. **2014**, 15(9), 2021-2026

[20] Song, C.K.; Luck, K.A.; Zhou, N.; Zeng, L.; Heitzer, H.M.; Manley, E.F.; Goldman, S.; Chen, L.X.; Ratner, M.A.; Bedzyk, M.J.; Chang, R.P.H.; Hersam, M.C.; Marks, T.J. "Supersaturated" Self-Assembled Charge-Selective Interfacial Layers for Organic Solar Cells. JACS **2014**, 136(51), 17762-17773

[21] Rozsnyai, L. F.; Wrighton, M. S. Selective Electrochemical Deposition of Polyaniline via Photopatterning of a Monolayer-modified Substrate. J. Am. Chem. Soc. **1994**, 116(13), 5993-5994

[22] Rozsnyai, L. F.; Wrighton, M. S. Controlling the adhesion of conducting polymer films with patterned self-assembled monolayers. Chem. Mater. **1996**, 8(2), 309

[23] Sayre, C. N.; Collard, D. M. Deposition of Polyaniline on Micro-contact Printed Self-assembled Monolayers of Omega-functionalized Alkanethiols. J. Mater. Chem., **1997**, 7(6), 909–912

[24] Kemp, N. T.; McGrouther, D.; Cochrane, J. W.; Newbury, R. Bridging the Gap: Polymer Nanowire Devices. Adv. Mater., **2007**, 19 (18), 2634-2638

[25] Kemp, N. T.; Cochrane, J. W.; Newbury, R. Patterning of Conducting Polymer Nanowires on Gold/Platinum Electrodes. Nanotech. **2007**, 18 (14), 145610-145617

[26] Kemp, N. T.; Newbury, R.; Cochrane, J. W.; Dujardin, E. Electronic Transport in Conducting Polymer Nanowire Array Devices. Nanotech. **2011**, 22(10), 105202-105205

[27] Hao, Q.; Kulikov, V.; Mirsky, V. M. Investigation of contact and bulk resistance of conducting polymers by simultaneous two- and four-point technique. Sensors and Actuators B **2003,** 94, 352–357

[28] Chen, Y.; Shih, I. Effects of $FeCl_3$ doping on polymer-based thin film transistors. J. Appl. Phys. **2004**, 96(1), 454-458

[29] Mukherjee, A.K.; Thakur, A.K.; Takashima W.; Kaneto K. Minimization of contact resistance between metal and polymer by surface doping. J. Phys. D: Appl. Phys. **2007**, 40, 1789-1793

[30] Chen, Y.; Kang, E.T..; Neoh, K.G. Oxidative Graft Polymerization of Aniline on Modified Si(100) Surface. Macrmol. **2001**, 34, 3133-3141

[31] Zhu, F.; Low, B.; Zhang, K.; Chua, S. Lithium–fluoride-modified indium tin oxide anode for enhanced carrier injection in phenyl-substituted polymer electroluminescent devices. Appl. Phys. Lett., **2001**, 79(8), 1205-1207

[32] Shen, H.; Mark, J. E.; Seliskar, C.J.; Mark, H.B.; Heineman, W. R. Blocking Behavior of Self-Assembled Monolayers on Gold Electrodes. J. Solid. State. Electrochem **1997**, 1(2), 148-154

[33] Nath, C.; Kumar, A.; Syu, K.-Z.; Kuo, Y.-K. Heat Conduction in Conducting Polyaniline Nanofibers. Applied. Phys. Letts **2013**, 103(12) 121905

[34] de Albuquerque, E.; Melo, W. L. B.; Faria, R. M. Determination of Physical Parameters of Conducting Polymers by Photothermal Spectroscopies. Rev. Sci. Instrum. **2003**, 74 (1), 306-308

[35] Yan, H.; Sada, N.; Toshima, N. J. Thermal Transporting Properties of Electrically Conductive Polyaniline Films as Organic Thermoelectric Materials. J. Thermal Analysis Calorimetry **2002**, 69 (3), 881-887

[36] Jin, J.; Manoharan, M. P.; Wang, Q.; Haque, M. A. In-plane Thermal Conductivity of Nanoscale Polyaniline Thin Films. Appl. Phys. Letts. **2009**, 95(3), 033113

[37] Stejskal, J.; Gilbert, R. G. Polyaniline. Preparation of a conducting polymer (IUPAC technical report). Pure Appl. Chem., **2002**, 74(5), 857–867

[38] Cernuschi, F.; Russo, A.; Piana, G. M.; Mutti, P.; Viviani, L. Quantitative InfraRed Thermography. Eurotherm Series 50, Pisa (**1997**) Edizioni ETS

[39] Bain, C.D.; Troughton, E.B.; Tao, Y.T.; Evall, J.; Whitesides, G.M.; Nuzzo, R.G. Formation of Monolayer Films by the Spontaneous Assembly of Organic Thiols From Solution onto Gold. J. Am. Chem. Soc, **1989**, 111 (1), 321-335

[40] Love, J. C.; Estroff, L. A.; Kriebel, J. K.; Nuzzo, R. G.; Whitesides, G. M. Self-assembled monolayers of thiolates on metals as a form of nanotechnology. Chem. Reviews, **2005**, 105, 1103-1170

[41] Sayre, C. N.; Collard, D. M. Electrooxidative deposition of polypyrrole and polyaniline on self-assembled monolayer modified electrodes. Langmuir **1997**, 13(4), 714-722

[42] Gonçalves, D.; Irene, E. A. The protective nature of dodecanethiol self-assembled monolayers deposited on Au for the electropolymerization of 3-methylthiophene. Electroanalysis **2003**, 15(7), 652-658

[43] Mazur M.; Krysiński, P. Comparative study of the electrodeposition of poly(3-octylthiophene) films on gold electrodes: Bare and modified with dodecanethiol monomolecular layer. Langmuir **2000**, 16(21), 7962-7967

[44] Sabatani, E.; Gafni, Y.; Rubinstein I. Morphology Control in Electrochemically Grown Conducting Polymer-Films 3. A Comparitive-Study of Polyaniline Films on Bare and on Gold Pretreated with p-Aminothiophenol. J. Phys. Chem. **1995**, 99 (32), 12305-12311

[45] Kemp, N.T.; Cochrane J.W.; Newbury R. Characteristics of the Nucleation and Growth of Template-free Polyaniline Nanowires and Fibrils. Synth. Metals **2009**, 159(5-6), 435-444

[46] Boudinet, D.; Benwadih, M.; Qi, Y.B.; Altazin, S.; Verilhac, J.M.; Kroger, M.; Serbutoviez, C.; Gwoziecki, R. ; Coppard, R.; Blevennec, G.L.; Kahn, A.; Horowitz, G. Modification of gold source and drain electrodes by self-assembled monolayer in staggered n- and p-channel organic thin film transistors. Organic Electronics **2010**, 11(2), 227–237

[47] Stafström, S.; Brédas, J.L.; Epstein, A.J.; Woo, H.S.; Tanner, D.B.; Huang, W.S.; MacDiarmid, A.G. Polaron Lattice in Highly Conducting Polyaniline: Theoretical and Optical Studies, Phys. Rev. Letts, **1987**, 59(13), 1464-1467

[48] McCall, R. P.; Ginder, J. M.; Leng, J. M.; Ye, H. J.; Manohar, S.K.; Masters, J. G.; Asturias, G. E.; MacDiarmid, A. G.; Epstein, A. J. Spectroscopy and defect states in polyaniline. Phys. Rev. B **1990**, 41, 5202-5213

[49] Liess, M.; Chinn, D., Petelenz. D.; Janata, J. Properties of insulated gate field-effect transistors with a polyaniline gate, Thin Solid Films **1996**, 286, 252-255

[50] Misra, S.C.K.; Ram, M.K.; Pandey S.S.; Malhotra B.D.; Chandra S. Vacuum-deposited metal/polyaniline Schottky device. Appl. Phys. Letts **1992**, 61(10), 1219-1221

[51] Kuo, C.-T.; Chiou, W.-H. Field-effect transistor with polyaniline thin film as semiconductor, Synthetic Metals, **1997**, 88, 23-30

[52] Kemp, N.T.; Kaiser, A.B.; Liu, C. J.; Chapman, B.; Mercier, O.; Carr, A.M; Trodahl, H. J.; Buckley, R.G.; Partridge, A.C.; Lee, J.Y.; Kim, C.Y.; Bartl, A.; Dunsch, L.; Smith, W.T.; Shapiro, J. S.; Thermoelectric Power and Conductivity of Different Types of Polypyrrole. J. of Polym. Sci. **1999**, 37(9), 953-960

[53] Sanjai, B.; Raghunathan, A.; Natarajan, T. S.; Rangarajan, G.; Thomas, S.; Prabhakaran, P. V.; Venkatachalam, S. Charge transport and magnetic properties in polyaniline doped with methane sulphonic acid and polyaniline-polyurethane blend. Phys. Rev. B **1997**, 55(16), 10734-10744

[54] Huang, J.; Wan, M.X. Polyaniline Doped with Different Sulfonic Acids by in situ Doping Polymerization. J. Polym. Sci. Pt A: Polym. Chem. **1999**, 37 (9), 1277–1284

[55] Xing, S.; Zhao, C.; Jing, S.; Wang, Z. Morphology and Conductivity of Polyaniline Nanofibers Prepared by 'Seeding' Polymerization. Polymer **2006**, 47(7), 2305-2313

[56] Huang J.; Kaner, R.B. A General Chemical Route to Polyaniline Nanofibers. J. Am. Chem. Soc. **2004**, 126 (3), 851-855

[57] Rahy, A.; Yang, D.J. Synthesis of Highly Conductive Polyaniline Nanofibers. Mats. Letts. **2008**, 62(28) 4311-4314

[58] Lee, K.; Cho, S.; Park, S.H.; Heeger, A.J.; Lee, C.-W.; Lee, S.-H. Metallic Transport in Polyaniline. Nature **2006**, 441 (7089), 65-68

[59] Nguyen, V.C.; Potje-Kamloth, K. Electrical and chemical sensing properties of doped polypyrrole / gold Schottky barrier diodes. Thin Solid Films, **1999**, 338(1-2), 142-148

[60] Campos, M.; Bulhões, L.O.S.; Lindino, C.A. Gas-sensitive characteristics of metal/semiconductor polymer Schottky device. Sensors and Actuators **2000**, 87, 67-71

TOC Graphic